

# Neutrino synchrotron emission from dense magnetized electron gas of neutron stars

V.G. Bezchastnov<sup>1</sup>, P. Haensel<sup>2</sup>, A.D. Kaminker<sup>1</sup>, and D.G. Yakovlev<sup>1</sup>

<sup>1</sup> A.F. Ioffe Physical Technical Institute, 194021 St. Petersburg, Russia

<sup>2</sup> N. Copernicus Astronomical Center, Polish Academy of Sciences, Bartycka 18, PL-00716 Warszawa, Poland

Received 14 March 1997 / Accepted 24 July 1997

**Abstract.** We study the synchrotron emission of neutrino pairs by relativistic, degenerate electrons in strong magnetic fields. Particular attention is paid to the case in which the dominant contribution comes from one or several lowest cyclotron harmonics. Calculations are performed using the exact quantum formalism and the quasiclassical approach. Simple analytic fits to the neutrino synchrotron emissivity are obtained in the domain of magnetized, degenerate and relativistic electron gas provided the electrons populate either many Landau levels or the ground level alone. The significance of the neutrino synchrotron energy losses in the interiors of cooling neutron stars is discussed.

**Key words:** dense matter – stars: interiors – stars: neutron – radiation mechanisms: non-thermal

---

## 1. Introduction

In this article, we study the synchrotron emission of neutrino pairs by relativistic, degenerate electrons in strong magnetic fields,

$$e \rightarrow e + \nu + \bar{\nu}. \quad (1)$$

This emission can be an important source of neutrino energy losses from the crusts of magnetized cooling neutron stars (NSs) as well as (in a modified form) from the superfluid NS cores.

The process has been considered by several authors starting from the pioneering article by Landstreet (1967). The adequate quasiclassical formalism was developed by Kaminker, Levenfish & Yakovlev (1991, hereafter KLY) who presented also critical analysis of preceding work. KLY carried out detailed analytic and numerical analysis of the case in which the electrons populated many Landau levels and the main contribution into the synchrotron emission came from high cyclotron harmonics. They also considered briefly the opposite case of the

superstrong magnetic field which suppresses greatly the contribution from all harmonics. In that case, only the first harmonics actually survives (although exponentially damped).

Exact quantum formalism of the neutrino synchrotron emission was developed by Kaminker et al. (1992a). Kaminker & Yakovlev (1993) considered the synchrotron process in the non-degenerate electron gas. Recently Kaminker et al. (1997) have analyzed how the synchrotron emission is modified in the superconducting NS cores where the initially uniform magnetic field splits into fluxoids. In a recent article, Vidaurre et al. (1995) have reconsidered the results of KLY claiming them to be inaccurate.

In the present article, we continue to study the neutrino synchrotron radiation from the degenerate magnetized electron gas. The emphasis is made upon the case in which the electron transitions associated with one or several lowest cyclotron harmonics are most important. This case has not been studied attentively earlier. We calculate the neutrino emissivity numerically using the exact quantum formalism (Sect. 2, Appendix A). We also use the quasiclassical approach (Sect. 3, Appendix B), combine our new results with those by KLY and propose an analytic fit that describes accurately all the neutrino synchrotron radiation regimes in a strongly degenerate, relativistic electron gas in which the electrons occupy many Landau levels. Another limiting case in which the electrons populate the ground level alone is considered in Appendix C. In Sect. 3 we present also critical discussion of the results by Vidaurre et al. (1995). In Sect. 4 we show the importance of the neutrino synchrotron emission in the NS interiors.

## 2. Quantum formalism

We will mainly use the units in which  $m_e = c = \hbar = k_B = 1$ , where  $k_B$  is the Boltzmann constant. We will return to ordinary physical units whenever necessary. The general expression for the neutrino synchrotron energy loss rate (emissivity, ergs  $s^{-1} cm^{-3}$ ) from an electron gas of any degeneracy and relativity, immersed in a quantizing magnetic field, was obtained by Kaminker et al. (1992a):

$$Q_{\text{syn}} = \frac{G_F^2 b}{3(2\pi)^5} \sum_{n=1, n'=0}^{\infty} \int_{-\infty}^{\infty} dp_z \int dq_z \int q_{\perp} dq_{\perp} \times A \omega f(1 - f'). \quad (2)$$

Here,  $G_F = 1.436 \times 10^{-49}$  ergs cm<sup>3</sup> is the Fermi weak-coupling constant and  $b = B/B_c$  is the dimensionless magnetic field ( $B_c = m_e^2 c^3 / (\hbar e) \approx 4.414 \times 10^{13}$  G). Furthermore,  $n$  and  $p_z$  are, respectively, the Landau level number and the momentum along the magnetic field for an electron before a neutrino-pair emission; the energy of this electron is  $\varepsilon = \sqrt{1 + 2nb + p_z^2}$ . The primed quantities  $n'$  and  $p'_z$  refer to an electron after the emission; its energy is  $\varepsilon' = \sqrt{1 + 2n'b + p_z'^2}$ ;  $f = f(\varepsilon) = \{\exp[(\varepsilon - \mu)/T] + 1\}^{-1}$  is Fermi-Dirac distribution of the initial-state electrons,  $f' = f(\varepsilon')$  is the same for the final-state electrons;  $\mu$  is the electron chemical potential and  $T$  is the temperature. The energy and momentum carried away by a neutrino-pair are denoted as  $\omega = \varepsilon - \varepsilon'$  and  $\mathbf{q}$ , respectively. The  $z$  component of  $\mathbf{q}$  is  $q_z = p_z - p'_z$ , while the component of  $\mathbf{q}$  across the magnetic field is denoted by  $q_{\perp}$ . The summation and integration in (2) is over all allowed electron transitions. The integration has to be done over the kinematically allowed domain  $q_z^2 + q_{\perp}^2 \leq \omega^2$ . The differential transition rate  $A$  (summed over initial and final electron spin states) is given by Eq. (17) of Kaminker et al. (1992a). Taking into account that some terms are odd functions of  $p_z$  and vanish after the integration, we can rewrite  $A$  in a simple form,

$$A = \frac{C_+^2}{2\varepsilon\varepsilon'} \left\{ [(\omega^2 - q_z^2 - q_{\perp}^2)(p_{\perp}^2 + p_{\perp}'^2 + 2) + q_{\perp}^2] (\Psi - \Phi) - (\omega^2 - q_z^2 - q_{\perp}^2)^2 \Psi + (\omega^2 - q_z^2 - q_{\perp}^2) \Phi \right\} - \frac{C_-^2}{2\varepsilon\varepsilon'} [(2\omega^2 - 2q_z^2 - q_{\perp}^2) (\Psi - \Phi) + 3(\omega^2 - q_z^2 - q_{\perp}^2) \Phi]. \quad (3)$$

Here,  $p_{\perp} = \sqrt{2nb}$  and  $p'_{\perp} = \sqrt{2n'b}$  are the transverse momenta of the initial-state and final-state electrons, respectively;

$$\Psi = F_{n'-1, n}^2(u) + F_{n', n-1}^2(u), \quad \Phi = F_{n'-1, n-1}^2(u) + F_{n', n}^2(u), \quad (4)$$

$u = q_{\perp}^2 / (2b)$ ,  $F_{n'n}(u) = (-1)^{n'-n} F_{nn'}(u) = u^{(n-n')/2} e^{-u/2} (n'!/n!)^{1/2} L_{n'-n}^{n-n'}(u)$ , and  $L_n^s(u)$  is an associated Laguerre polynomial (see, e.g., Kaminker & Yakovlev 1981). Furthermore, in Eq. (3) we introduce  $C_+^2 = \sum_{\nu} (C_V^2 + C_A^2)$  and  $C_-^2 = \sum_{\nu} (C_V^2 - C_A^2)$ , where  $C_V$  and  $C_A$  are the vector and axial vector weak interaction constants, respectively, and summation is over all neutrino flavors. For the emission of the muonic or tauonic neutrinos (neutral currents only),  $C_V' = 2 \sin^2 \theta_W - 0.5$  and  $C_A' = -0.5$ ;  $\theta_W$  is the Weinberg angle. Adopting  $\sin^2 \theta_W \simeq 0.23$  we obtain  $C_+^2 \approx 1.675$  and

$C_-^2 \approx 0.175$ . A comparison of the neutrino synchrotron emission by electrons with the familiar electromagnetic synchrotron emission has been done by KLY. Although electromagnetic radiation is much more intense it does not emerge from deep neutron star layers (neutron star interior is opaque to photons) while neutrino emission escapes freely from stellar interior, producing an efficient internal cooling.

We have composed a computer code which calculates  $Q_{\text{syn}}$  from Eqs. (2) and (3) for arbitrary plasma parameters  $\rho Y_e$ ,  $T$  and  $B$ , where  $\rho$  is the mass density and  $Y_e$  is the number of electrons per baryon. Technical details are presented in Appendix A, the results are illustrated in Sect. 4, and the case of very strong magnetic field, in which the bulk of electrons occupy the ground Landau level, is considered in Appendix C.

### 3. Quasiclassical treatment

In this section, we develop quasiclassical description of the neutrino synchrotron emission from a degenerate, ultrarelativistic electron gas in a strong magnetic field  $B = 10^{11}$ - $10^{14}$  G. Therefore we assume that  $\mu \gg m_e c^2$  and  $T \ll T_F$ , where  $T_F = (\mu - m_e c^2) / k_B \approx \mu / k_B$  is the degeneracy temperature. We mainly analyze the case in which the electrons populate many Landau levels. This is so if the magnetic field is nonquantizing or weakly quantizing (e.g., Kaminker & Yakovlev, 1994), i.e., if  $\mu \gg \sqrt{1 + 2b}$ . The latter condition is realized at sufficiently high densities  $\rho \gg \rho_B$ , where  $\rho_B \approx 2.07 \times 10^6 b^{3/2} / Y_e$  g cm<sup>-3</sup> =  $2.23 \times 10^5 B_{13}^{3/2} / Y_e$  g cm<sup>-3</sup>, and  $B_{13} = B / (10^{13}$  G). At these densities,  $\mu$  is nearly the same as without magnetic field,  $\mu \approx c p_F \approx \hbar (3\pi^2 n_e)^{1/3}$ , where  $p_F$  is the field-free Fermi momentum. The formulated conditions are typical for the neutron star crusts.

In the case of many populated Landau levels, we can replace the summation over  $n$  by the integration over  $p_{\perp}$  in Eq. (2). The remaining summation over  $n'$  can be conveniently replaced by the summation over discrete cyclotron harmonics  $s = n - n' = 1, 2, 3, \dots$ . Furthermore, an initial-state electron can be described by its quasiclassical momentum  $p$  and pitch-angle  $\theta$  ( $p_z = p \cos \theta$ ,  $p_{\perp} = p \sin \theta$ ). Since we consider strongly degenerate electrons we can set  $\varepsilon = \mu$  and  $p = p_F$  in all smooth functions under the integrals. Then the integration over  $p$  is done analytically. In this way we transform the rigorous quantum formalism of Sect. 2 to the quasiclassical approximation used by KLY (see their Eqs. (3), (4) and (8)).

According to KLY the quasiclassical neutrino synchrotron emission is different in three temperature domains  $\mathcal{A}$ ,  $\mathcal{B}$ , and  $\mathcal{C}$  separated by two typical temperatures  $T_P$  and  $T_B$ :

$$T_P = \frac{3\hbar\omega_B^* x^3}{2k_B} = \frac{3}{2} T_B x^3 \approx 2.02 \times 10^9 B_{13} x^2 \text{ K}, \quad T_B = \frac{\hbar\omega_B^*}{k_B} \approx 1.34 \times 10^9 B_{13} (1 + x^2)^{-1/2} \text{ K}. \quad (5)$$

Here,  $x = p_F / (m_e c)$  is the relativistic parameter ( $x \gg 1$ , in our case), and  $\omega_B^* = eBc / \mu$  is the electron gyrofrequency at the Fermi surface. Notice, that while applying our results to the

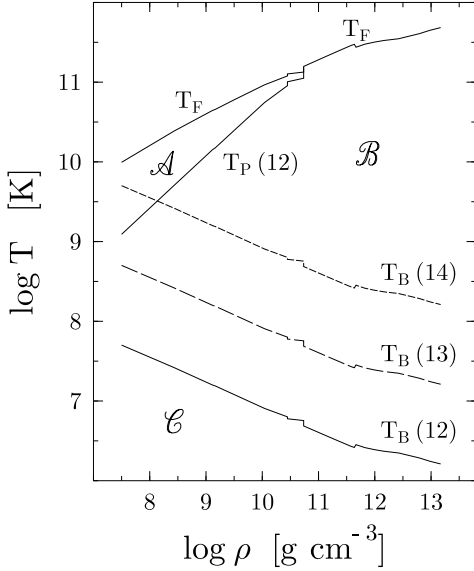


**Fig. 1.** Density-temperature domains of different neutrino synchrotron regimes.  $T_B$  is temperature (5) below which (domain  $\mathcal{C}$ ) the emission goes via the ground cyclotron harmonics  $s = 1$  (for  $B = 10^{12}$ ,  $10^{13}$  and  $10^{14}$  G,  $\log B$  shown in parenthesis).  $T_P$  is temperature (5) below which (in domain  $\mathcal{B}$ ) the Pauli principle restricts the number of cyclotron harmonics (see text); it is shown only for  $B = 10^{12}$  G because  $T_P$  becomes higher than the electron degeneracy temperature  $T_F$  for  $B = 10^{13}$  and  $10^{14}$  G. Domain  $\mathcal{A}$  ( $T_P \ll T \ll T_F$ ) is realized only for  $B = 10^{12}$  G;  $T_F$  is independent of  $B$ , for displayed parameters.

neutron star crusts, one can use a simplified expression  $x \approx 1.009(\rho_6 Y_e)^{1/3}$ , where  $\rho_6 = \rho/(10^6 \text{ g cm}^{-3})$ .

Figure 1 demonstrates the main parameter domains  $\mathcal{A}$ ,  $\mathcal{B}$  and  $\mathcal{C}$  for the ground-state (cold catalyzed) matter of NS crusts. Thermal effects on the nuclear composition are neglected which is justified as long as  $T \lesssim 5 \times 10^9$  K (e.g., Haensel et al. 1996). It is assumed that nuclei of one species are available at any fixed density (pressure). Then the increase of density (pressure) is accompanied by jumps of nuclear composition (e.g., Haensel et al. 1996). The ground-state matter in the outer NS crust, at densities below the neutron drip density ( $4 \times 10^{11} \text{ g cm}^{-3}$ ), is described using the results by Haensel & Pichon (1994) based on new laboratory measurements of masses of neutron-rich nuclei. At higher densities, in the inner NS crust, we use the results of Negele & Vautherin (1973) derived on the basis of a modified Hartree-Fock method. Small discontinuities of the curves in Fig. 1 are due to the jumps of the nuclear composition. Notice, that the properties of the neutrino synchrotron emission vary rather smoothly in the transition regions from domain  $\mathcal{A}$  to  $\mathcal{B}$  and from  $\mathcal{B}$  to  $\mathcal{C}$ .

The *high-temperature* domain  $\mathcal{A}$  is defined as  $T_P \ll T \ll T_F$ ; it is realized for not too high densities and magnetic fields where  $T_P \ll T_F$ . In Fig. 1, this domain exists only for  $B = 10^{12}$  G at  $\rho < 10^{11} \text{ g cm}^{-3}$ . In domain  $\mathcal{A}$ , the degenerate electrons emit neutrinos through many cyclotron harmonics; typical harmonics is  $s \sim x^3$ . Corresponding neutrino energies  $\omega \sim \omega_B^* x^3 \ll T$  are not restricted by the Pauli principle. The

quasiclassical approach of KLY yields

$$Q_{\text{syn}}^{\mathcal{A}} = \frac{2}{189\pi^5} \frac{G_F^2 k_B T m_e^2 \omega_B^6 x^8}{c^5 \hbar^4} (25C_+^2 - 21C_-^2) \approx 3.09 \times 10^{15} B_{13}^6 T_9 x^8 \text{ ergs cm}^{-3} \text{ s}^{-1}, \quad (6)$$

where  $T_9 = T/(10^9 \text{ K})$ . Here and in what follows, numerical factors in the practical expressions are slightly different from those presented by KLY because now we use more accurate value of the Fermi constant (see Eq. (2)).

The *moderate-temperature* domain  $\mathcal{B}$  is defined as  $T_B \lesssim T \ll T_P$  and  $T \ll T_F$ . It covers wide temperature and density ranges (Fig. 1) most important for applications. In this domain, neutrinos are again emitted through many cyclotron harmonics  $s \sim k_B T / \hbar \omega_B^* \gg 1$ , but their spectrum is restricted by the Pauli principle, and typical neutrino energies are  $\omega \sim k_B T$ . As shown by KLY, in this case the neutrino emissivity is remarkably independent of the electron number density:

$$Q_{\text{syn}}^{\mathcal{B}} = \frac{2\zeta(5)}{9\pi^5} \frac{G_F^2 m_e^2 \omega_B^2}{c^5 \hbar^8} C_+^2 (k_B T)^5 \approx 9.04 \times 10^{14} B_{13}^2 T_9^5 \text{ ergs cm}^{-3} \text{ s}^{-1}, \quad (7)$$

where  $\zeta(5) \approx 1.037$  is the value of the Riemann zeta function.

The third, *low-temperature* domain  $\mathcal{C}$  corresponds to temperatures  $T \lesssim T_B$  at which the main contribution into the neutrino synchrotron emission comes from a few lower cyclotron harmonics  $s=1, 2, \dots$ . If  $T \ll T_B$ , even the first harmonics  $s = 1$  appears to be exponentially suppressed as discussed by KLY. A more detailed analysis will be given below.

The emissivity  $Q_{\text{syn}}^{\mathcal{AB}}$  in the combined domain  $\mathcal{A} + \mathcal{B}$ , including a smooth transition from  $\mathcal{A}$  to  $\mathcal{B}$  at  $T \sim T_P$ , was calculated accurately in KLY. The results (Eqs. (13), (15) and (18) in KLY), valid at  $T_B \lesssim T \ll T_F$ , can be conveniently rewritten as

$$Q_{\text{syn}}^{\mathcal{AB}} = Q_{\text{syn}}^{\mathcal{B}} S_{\mathcal{AB}}, \quad (8)$$

$$S_{\mathcal{AB}} = \frac{27\xi^4}{\pi^2 2^9 \zeta(5)} \left[ F_+(\xi) - \frac{C_-^2}{C_+^2} F_-(\xi) \right], \quad (9)$$

$$\xi \equiv \frac{T_P}{T} = \frac{3}{2} z x^3; \quad z = \frac{T_B}{T},$$

where the analytic fits to the functions  $F_{\pm}(\xi)$  read

$$F_+(\xi) = D_1 \frac{(1 + c_1 y_1)^2}{(1 + a_1 y_1 + b_1 y_1^2)^4},$$

$$F_-(\xi) = D_2 \frac{1 + c_2 y_2 + d_2 y_2^2 + e_2 y_2^3}{(1 + a_2 y_2 + b_2 y_2^2)^5}. \quad (10)$$

In this case  $y_{1,2} = [(1 + \alpha_{1,2} \xi^{2/3})^{2/3} - 1]^{3/2}$ ,  $a_1 = 2.036 \times 10^{-4}$ ,  $b_1 = 7.405 \times 10^{-8}$ ,  $c_1 = 3.675 \times 10^{-4}$ ,  $a_2 = 3.356 \times 10^{-3}$ ,  $b_2 = 1.536 \times 10^{-5}$ ,  $c_2 = 1.436 \times 10^{-2}$ ,  $d_2 = 1.024 \times 10^{-5}$ ,  $e_2 = 7.647 \times 10^{-8}$ ,  $D_1 = 44.01$ ,  $D_2 = 36.97$ ,  $\alpha_1 = 3172$ ,  $\alpha_2 = 172.2$ .

Now let us study the neutrino emissivity in the combined domain  $\mathcal{B} + \mathcal{C}$ . Using the quasiclassical expressions of KLY in the ultrarelativistic limit ( $m_e \rightarrow 0$ ) we obtain

$$Q_{\text{syn}}^{\text{BC}} = Q_{\text{syn}}^{\text{B}} S_{\text{BC}}, \quad (11)$$

where

$$S_{\text{BC}} = \frac{3}{2^6 \zeta(5)} \frac{1}{z^2 T^7} \sum_{s=1}^{\infty} \int_0^{\pi} \sin^3 \theta \, d\theta \int q_{\perp} \, dq_{\perp} \times \int dq_z (\omega^2 - q_z^2 - q_{\perp}^2) (\Psi - \Phi) \frac{\omega^2}{e^{\omega/T} - 1} \quad (12)$$

with

$$\Psi - \Phi = 2 \left[ \left( \frac{s^2}{y^2} - 1 \right) J_s^2(y) + J_s'^2(y) \right]. \quad (13)$$

Here,  $J_s(y)$  is a Bessel function of argument  $y = p_{\perp} q_{\perp} c / (eB)$ , and  $J_s'(y) = dJ_s(y)/dy$ . The neutrino-pair energy can be expressed as  $\omega \approx q_z \cos \theta + s\omega_B^*$ . The integration should be done over the kinematically allowed domain:  $\kappa_{\perp}^2 \geq q_{\perp}^2 + \sin^2 \theta (\kappa_z - q_z)^2$ ,  $\kappa_{\perp} = s\omega_B^* / \sin \theta$ ,  $\kappa_z = s\omega_B^* \cos \theta / \sin^2 \theta$ .

One can easily see that  $S_{\text{BC}}$  depends on the only parameter  $z$ . The domain  $\mathcal{B}$  corresponds to  $x^{-3} \ll z \ll 1$  while the domain  $\mathcal{C}$  corresponds to  $z \gtrsim 1$ . Equation (12), in which we set  $m_e \rightarrow 0$ , does not reproduce the high-temperature domain  $\mathcal{A}$ . However, we have already described the transition from  $\mathcal{B}$  to  $\mathcal{A}$  by Eqs. (8-10).

At  $z \ll 1$ , the neutrino emissivity, determined by  $S_{\text{BC}}$  in Eq. (12), comes from many cyclotron harmonics (see KLY, for details). A Bessel function  $J_s(y)$  and its derivative can be replaced by McDonald functions. The main contribution to the integrals (12) comes from a narrow vicinity  $|\kappa_{\perp} - q_{\perp}| \lesssim \omega_B^* s^{1/3}$ , and  $|q_z - \kappa_z| \lesssim \omega_B^* s^{2/3}$  of the saddle point  $q_{\perp} = \kappa_{\perp}$  and  $q_z = \kappa_z$ , in which the neutrino-pair energy is nearly constant,  $\omega \approx s\omega_B^* / \sin^2 \theta$ . Adopting these approximations and replacing the sum over  $s$  by the integral we reproduce evidently the result of KLY,  $S_{\text{BC}} = 1$ . However if we take into account small corrections in the expression of a Bessel function through McDonald functions (Sokolov & Ternov 1974), and weak variation of  $\omega$  near the saddle-point, we obtain a more accurate asymptote  $S_{\text{BC}} = 1 - 0.4535 z^{2/3}$ . The derivation is outlined in Appendix B.

In the opposite limit of  $z \gg 1$ , one can keep the contribution from the first harmonics  $s = 1$ , and replace  $(\Psi - \Phi) \rightarrow 1$ ,  $(e^{\omega/T} - 1)^{-1} \rightarrow e^{-\omega/T}$  in Eq. (12) as described in KLY. At any kinematically allowed  $q_z$  and  $q_{\perp}$ , the neutrino-pair emission is suppressed by a small factor  $\sim e^{-\omega/T}$ . As shown in KLY, the most efficient neutrino synchrotron radiation occurs from a small vicinity of the allowed region, where  $q_z \approx -\omega_B^* / (1 + \cos \theta)$  has minimum and the neutrino energy  $\omega \approx \omega_B^* / (1 + \cos \theta)$  is most strongly reduced by the quantum recoil effect. This region corresponds to the backward electron scattering. The integration over  $q_{\perp}$  is then done analytically, and

we are left with a two-fold integration over  $q_z$  and  $\theta$ . In the limit of very high  $z$ , it gives

$$S_{\text{BC}} \approx \frac{3}{2\zeta(5)} \exp\left(-\frac{z}{2}\right) \left(1 + \frac{28}{z}\right). \quad (14)$$

The convergence of this asymptote is very slow, and we present the second-order correction term  $28/z$  which improves the convergence considerably. For instance, at  $z = 60$  the two-term asymptote gives an error of about 6.5%, while the one-term asymptote gives an error of about 36%.

Notice, that the emissivity given by Eq. (20) in KLY in the limit of  $z \gg 1$  is 4 times smaller than the correct emissivity presented here (due to a simple omission in evaluating  $Q_{\text{syn}}^{\text{C}}$  made by KLY). Thus Eqs. (20) and (21) in KLY are inaccurate at  $z \gg 1$ .

In addition to analyzing the asymptotes, we have calculated  $S_{\text{BC}}$  numerically from Eq. (12) in the quasiclassical approximation at intermediate  $z$ . The results are fitted by the analytic expression

$$S_{\text{BC}} = \exp(-z/2) D_1(z) / D_2(z), \quad (15)$$

where  $D_1(z) = 1 + 0.4228 z + 0.1014 z^2 + 0.006240 z^3$ ,  $D_2(z) = 1 + 0.4535 z^{2/3} + 0.03008 z - 0.05043 z^2 + 0.004314 z^3$ . The fit reproduces both the low- $z$  and the high- $z$  asymptotes. The rms fit error at  $z \leq 70$  is about 1.6%, and the maximum error is 5% at  $z \approx 18$ .

Now, we can easily combine Eqs. (8) and (11) and obtain a general fit expression for the neutrino synchrotron emissivity which is valid everywhere in domains  $\mathcal{A}$ ,  $\mathcal{B}$ ,  $\mathcal{C}$  ( $T \ll T_F$ ,  $\rho \gg \rho_B$ ), where the electrons are degenerate, relativistic and populate many Landau levels:

$$Q_{\text{syn}}^{\text{ABC}} = Q_{\text{syn}}^{\text{B}} S_{\text{AB}} S_{\text{BC}}. \quad (16)$$

Here,  $Q_{\text{syn}}^{\text{B}}$  is given by Eq. (7), while  $S_{\text{AB}}$  and  $S_{\text{BC}}$  are defined by Eqs. (9), (10) and (15).

The neutrino synchrotron emission in domains  $\mathcal{B} + \mathcal{C}$  (in our notations), has been reconsidered recently by Vidaurre et al. (1995). Their results are compared with ours in Fig. 2 which shows the neutrino synchrotron emissivity as a function of  $B$  for the same plasma parameters ( $\rho Y_e = 10^{11} \text{ g cm}^{-3}$ ,  $T = 10^9 \text{ K}$ ) as in Fig. 4 by Vidaurre et al. (1995). For the parameters chosen (due to very high  $\rho$ ), domain  $\mathcal{A}$  is not realized, while the transition from domain  $\mathcal{B}$  to  $\mathcal{C}$  occurs at fairly high  $B$  (for instance,  $z = 1$  corresponds to  $B \approx 3.5 \times 10^{14} \text{ G}$ ). Our quasiclassical calculation, analytic fit (16) and quantum calculation are so close that yield the same (solid) line. Numerical calculation of Vidaurre et al. (1995) is shown by dashes, and their analytical approximation (claimed to be accurate at intermediate  $z$ ) by dots. In our notations, the latter approximation reads  $S_{\text{BC}}^{(\text{V})} = 0.0073 z^5 e^{-z}$ . We see that such an approximation reproduces neither low- $z$  nor high- $z$  asymptote, and is, in fact, inaccurate at intermediate  $z$ . It also disagrees with numerical curve of Vidaurre et al. (1995) and with our curve. The numerical results by Vidaurre et al. (1995) are considerably different from ours except at

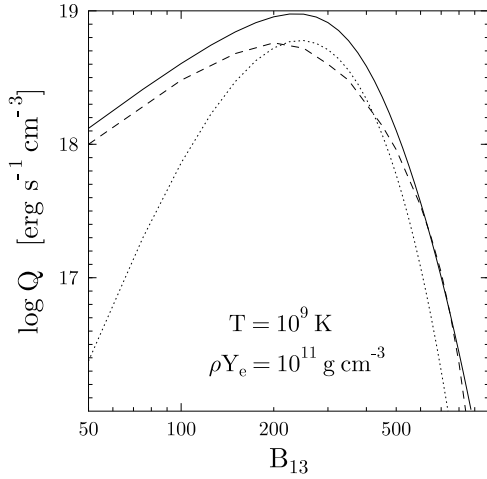


**Fig. 2.** Neutrino synchrotron emissivity vs  $B$  from a plasma with  $\rho Y_e = 10^{11} \text{ g cm}^{-3}$  and  $T = 10^9 \text{ K}$ . Solid curve shows our quasi-classical result, dash-curve – calculation of Vidaurre et al. (1995), dots – analytic Eq. (26) of these authors.

$B \approx (6 - 8) \times 10^{15} \text{ G}$ . At lower and higher  $B$  the disagreement becomes substantial. In domain  $\mathcal{B}$ , Vidaurre et al. (1995) present another analytic expression that differs from Eq. (7) by a numerical factor  $9/(2\pi)$ . The difference comes from two inaccuracies made by Vidaurre et al. (1995). First, while deriving the emissivity, they use the asymptote of the McDonald function at large argument (their Eq. (19)) instead of exact expression for the McDonald function (as was done by KLY). One can easily verify that this inaccuracy yields an extra factor  $3/\pi$ . Secondly, Vidaurre et al. (1995) calculated inaccurately an integral over  $q_z$  (their Eq. (22)) as if the integrand were independent of  $q_z$ . This yields the second extra factor  $3/2$ . Thus we can conclude that the results by Vidaurre et al. (1995) are rather inaccurate in a wide parameter range. We have performed extensive comparison of the results obtained with our quantum code and with the quasi-classical approach. We have found very good agreement (within 3-5 %) in all the cases in which the quasi-classical approach can be used (see above). This statement is illustrated in Figs. 3 and 4. Figure 3 shows the quantum and quasi-classical synchrotron emissivities from a plasma with  $\rho Y_e = 10^8 \text{ g cm}^{-3}$  and  $T = 10^9 \text{ K}$  as a function of  $B$ . Figure 4 displays the ratio of the quantum to quasi-classical emissivities in more detail. The quasi-classical approach is valid as long as  $\rho \gg \rho_B$  (as long as electrons populate many Landau levels) which corresponds to  $B \ll 6 \times 10^{14} \text{ G}$  for our particular parameters. For these magnetic fields, the quantum and quasi-classical results are seen to coincide quite well. Low-amplitude oscillations of the curves in Fig. 4 reflect oscillations of the synchrotron emissivity as calculated with the quantum code. The oscillations are produced by depopulation of higher Landau levels with increasing  $B$ . They represent quantum effect associated with square-root singularities of the Landau states. As seen from Fig. 4 the oscillations are smeared out with increasing  $T$  by thermal broadening of the square-root singularities (cf. Yakovlev & Kaminker 1994).

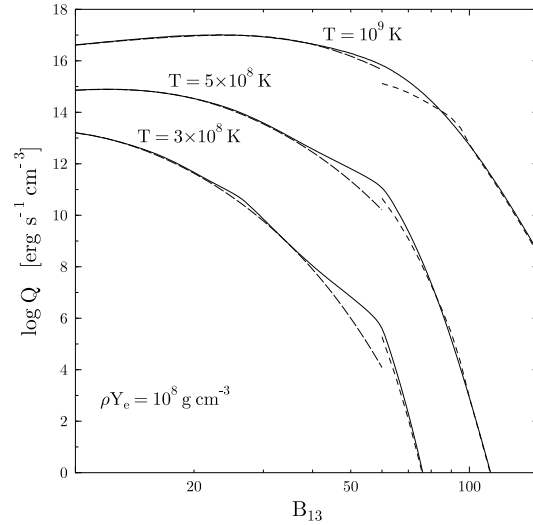


**Fig. 3.** Neutrino synchrotron emissivity versus  $B$  from a plasma with  $\rho Y_e = 10^8 \text{ g cm}^{-3}$  at  $T = 3 \times 10^8, 5 \times 10^8$  and  $10^9 \text{ K}$ . Solid curves are calculated with the quantum code, long-dash-curves are obtained using the quasi-classical calculation valid at  $B \ll 6 \times 10^{14} \text{ G}$ , dash-curves show the quantum asymptotic expression (Appendix C) for the case in which the ground Landau level is populated alone,  $B > 6 \times 10^{14} \text{ G}$ .

In a higher field  $B \gtrsim 6 \times 10^{14} \text{ G}$ , the electrons populate the ground Landau level alone and the electron chemical potential is reduced by the magnetic field. Very high  $B$ , not shown in Fig. 3, remove the electron degeneracy. Note that at high temperatures, one should take into account the synchrotron neutrino emission by positrons (Kaminker & Yakovlev 1994). All these conditions are described by the quantum code while the quasi-classical approach is no longer valid. In Appendix C, we obtain simple asymptotic expressions for  $Q_{\text{syn}}$  in the case in which the electrons populate the ground Landau level alone. Corresponding curves are shown by dashed curves in Fig. 3, and they are seen to reproduce the exact quantum curves quite accurately.

#### 4. Discussion and results

Figures 5-8 display density dependence of the neutrino synchrotron emissivity  $Q_{\text{syn}}$  calculated from Eq. (16) for the magnetic fields  $B = 10^{12}, 10^{13}$ , and  $10^{14} \text{ G}$  at four temperatures  $T = 3 \times 10^9, T = 10^9, 3 \times 10^8$ , and  $10^8 \text{ K}$ , respectively. We adopt the ground-state model of matter in the NS crust (see Sect. 3). Various neutrino-emission regimes can be understood by comparison with Fig. 1.

The high-density (horizontal) parts of the synchrotron curves correspond to domain  $\mathcal{B}$  (Eq. (7)), where  $Q_{\text{syn}}$  is density independent. The low-density bends are associated with transitions either into domain  $\mathcal{A}$  (where  $Q_{\text{syn}} \propto \rho^{8/3}$  according to Eq. (6)) or into domain  $\mathcal{C}$  (where  $Q_{\text{syn}}$  decreases exponentially due to cyclotron harmonics suppression, Eq. (14)). Domain  $\mathcal{A}$  is realized only for  $B = 10^{12} \text{ G}$  and  $T \gtrsim 10^9 \text{ K}$  in Figs. 5 and 6. The low-density bends of  $Q_{\text{syn}}$  in domain  $\mathcal{C}$  are much steeper than those in domain  $\mathcal{A}$ . These bends are more pronounced at

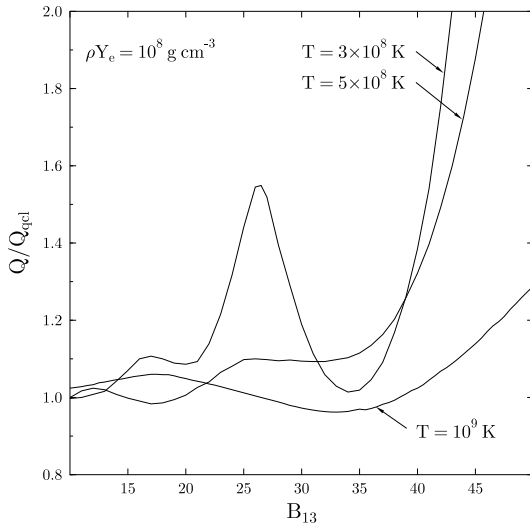


**Fig. 4.** Ratios of the quantum to quasiclassical neutrino synchrotron emissivities presented in Fig. 3.

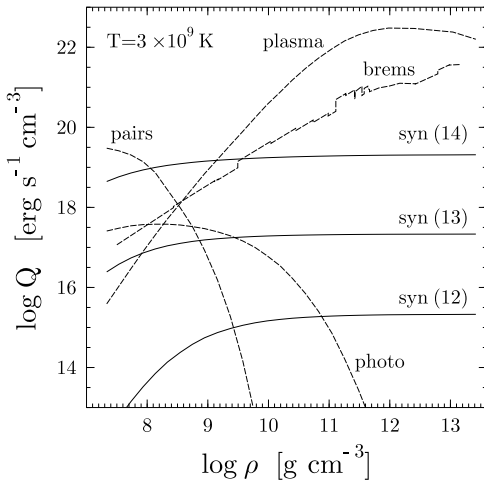


**Fig. 5.** Density dependence of neutrino emissivities from ground-state matter of the NS crust due to various mechanisms at  $T = 3 \times 10^9$  K. Curves ‘syn’ ‘(12)’, ‘(13)’, and ‘(14)’ refer to the synchrotron mechanism at  $B = 10^{12}$ ,  $10^{13}$  and  $10^{14}$  G, respectively. Curve ‘pairs’ corresponds to neutrino emission due to annihilation of electron-positron pairs; it is almost independent of  $B$  at given  $T$ . Other curves are for  $B = 0$ : ‘brems’ – the total electron-nucleus bremsstrahlung; ‘plasma’ – plasmon decay; ‘photo’ – photoneutrino process (see text).

highest  $B = 10^{14}$  G, at which domain  $\mathcal{E}$  extends to higher  $T$  and  $\rho$  (Figs. 7 and 8).

For comparison, we also plot the emissivities produced by other neutrino generation mechanisms: the electron-positron pair annihilation into neutrino pairs, electron-nucleus bremsstrahlung, plasmon decay and photon decay. The pair annihilation in a magnetized plasma has been considered by Kaminker et al. (1992a, b), and Kaminker & Yakovlev (1994). For the parameters of study, the emissivity appears to be weakly dependent on the magnetic field. At  $B \lesssim 10^{13}$  G it is very

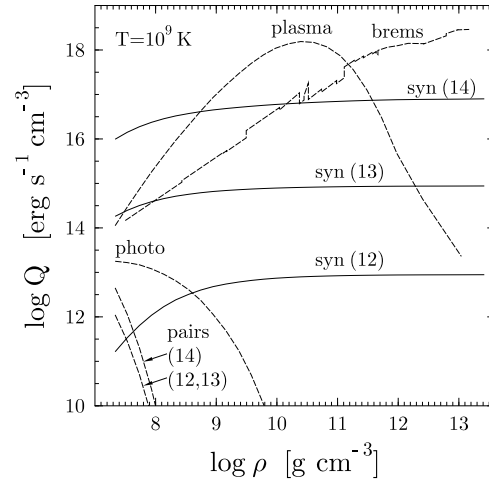


**Fig. 6.** Same as in Fig. 5 but at  $T = 10^9$  K. Pair annihilation depends noticeably on  $B$ .

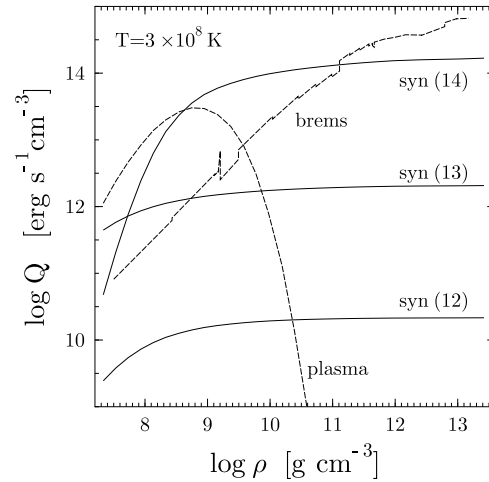


**Fig. 7.** Same as in Figs. 5 and 6 but at  $T = 3 \times 10^8$  K. Pair annihilation and photoneutrino processes become negligible.

close to the zero-field emissivity (Itoh et al. 1989, 1996). As seen from Figs. 5 and 6, the pair-annihilation emissivity differs slightly from the zero-field one only in a not too hot plasma ( $T \lesssim 10^9$  K) at  $B \gtrsim 10^{14}$  G. The neutrino bremsstrahlung curves are plotted neglecting the influence of the magnetic field. The effect of the field on the bremsstrahlung has not been studied so far but it is expected to be weak, for the parameters in Figs. 5-8. We use the results of Haensel et al. (1996) to describe the neutrino pair bremsstrahlung due to Coulomb scattering of electrons by atomic nuclei in the liquid phase of matter. In the solid phase, similar process is known to consist of two parts: the phonon and static lattice contributions. We use the results by Yakovlev & Kaminker (1996) to evaluate the phonon contribution. As for the static lattice contribution, we employ the most recent theory by Pethick & Thorsson (1996) and perform numerical calculation from Eqs. (28) and (29) of their paper (adopting the Debye-Waller factor and the nuclear form-factor

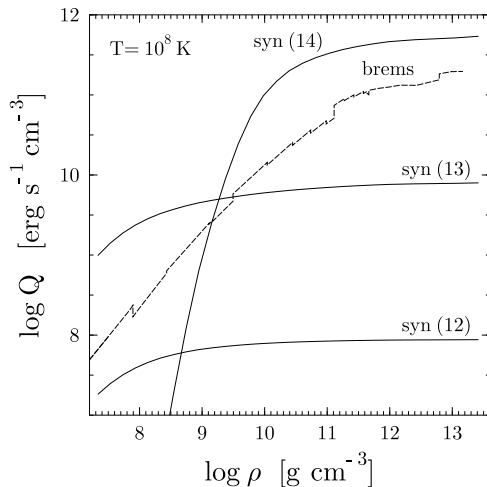


**Fig. 8.** Same as in Figs. 5 - 7 but at  $T = 10^8$  K. Plasmon decay becomes negligible.

which were used by Yakovlev & Kaminker 1996). Numerous jumps of the bremsstrahlung curves in Figs. 5-8 are associated either with jump-like changes of nuclear composition of cold-catalyzed matter or with solid-liquid phase transitions (see Haensel et al. 1996 for details). The neutrino emissivities from other processes are determined by the electron and positron number densities which are nearly continuous function of the density. Therefore, all other curves are smooth. The neutrino generation due to plasmon and photon decays in a magnetic field has not been considered in the literature, and we present the field-free results of Itoh et al. (1989, 1996), for illustration.

In the case of zero magnetic field, the bremsstrahlung process dominates completely in most dense layers of the NS crust at not too high temperatures  $T \lesssim 10^9$  K. Plasmon decay, photon decay, and pair annihilation are significant at high temperatures,  $T \gtrsim 10^9$  K, but their emissivities become negligible very soon as temperature decreases.

The synchrotron emissivity is, to some extent, similar to the bremsstrahlung, for it persists over the wide temperature and density ranges. In the presence of the strong magnetic field  $B \gtrsim 10^{13}$  G, the synchrotron emission is seen to be important and even dominant for any  $T$  in Figs. 5-8. In a hot plasma (Fig. 5), the synchrotron emission is significant at comparatively low densities,  $\rho = 10^8$ - $10^9$  g cm $^{-3}$ . With decreasing  $T$  the neutrino synchrotron emission becomes more important at higher densities. At  $T = 10^8$  K, only the bremsstrahlung and synchrotron emissions actually survive (Fig. 8); if  $B = 10^{14}$  G, the synchrotron emission dominates over the bremsstrahlung one in a wide density range,  $\rho \gtrsim 10^9$  g cm $^{-3}$ .

## 5. Conclusions

We have considered the synchrotron neutrino-pair emission of electrons from a dense magnetized plasma. We developed a computer code (Sect. 2) which calculates the synchrotron emission in the presence of quantizing magnetic fields for a wide

range of conditions at which the electrons can be weakly as well as strongly degenerate and/or relativistic. We have also calculated the synchrotron emissivity in the quasiclassical approximation (Sect. 3) for strongly degenerate, relativistic electrons which populate many Landau levels. We have paid special attention to the case in which the main contribution into the synchrotron neutrino emission comes from the fundamental or several low cyclotron harmonics. This case has not been analyzed properly earlier by KLY and Vidaurre et al. (1995). We have obtained a simple analytic expression (16) which fits accurately our quasiclassical results in wide ranges of densities, temperatures, and magnetic fields. In Sect. 4 we have demonstrated that the synchrotron neutrino emissivity gives considerable or even dominant contribution into the neutrino emissivity at  $B \gtrsim 10^{13}$  G in moderate-density and/or high-density layers of the NS crusts, depending on temperature and magnetic field. Let us notice, that the neutrino emissivities plotted in Figs. 5-8 are appropriate for cooling neutron stars rather than for newly born or merging neutron stars. Since the neutrino radiation from a cooling neutron star is too weak to be detected with modern neutrino observatories we do not calculate the spectrum of emitted neutrinos.

Our results indicate that the neutrino synchrotron emission should be taken into account in the cooling theories of magnetized neutron stars. It can be important during initial cooling phase ( $t = 10$ - $1000$  yrs after the neutron star birth). At this stage, the thermal relaxation of internal stellar layers is not achieved (e.g., Nomoto & Tsuruta 1987, Lattimer et al. 1994) and local emissivity from different crustal layers can affect this relaxation and observable surface temperature.

The synchrotron process in the crust can also be significant at the late neutrino cooling stages ( $t \sim 10^5$  yrs,  $T \sim 10^8$  K), in the presence of strong magnetic fields  $B \gtrsim 10^{14}$  G. The synchrotron emission can be the dominant neutrino production mechanism in the neutron star crust, while the neutrino luminosity from the stellar core may be not too high, at this cooling stage, and quite comparable with the luminosity from the crust.

It is worthwhile to mention that the synchrotron emission can be important also in the superfluid neutron star cores (Kaminker et al. 1997). A strong superfluidity of neutrons and protons suppresses greatly (e.g., Yakovlev & Levenfish 1995) the traditional neutrino production mechanisms such as Urca processes or nucleon-nucleon bremsstrahlung. The superfluidity (superconductivity) of protons splits an initial, locally uniform magnetic field of the neutron star core into fluxoids – thin magnetic threads of quantized magnetic flux. This process modifies the neutrino synchrotron process (Kaminker et al. 1997) amplifying it just after the superconductivity onset and making it significant since the traditional neutrino generation mechanisms are suppressed. It has been shown that this modified neutrino synchrotron process can dominate over other mechanisms if the initially uniform magnetic field in the NSs core is  $B \gtrsim 10^{13}$  G and if  $T \lesssim 5 \times 10^8$  K. These fields and temperatures are quite consistent with the results of the present article: similar conditions are necessary for the synchrotron emission to dominate over other neutrino production mechanisms in the NS crust by

the end of the neutrino cooling stage. If so, the total neutrino luminosity (from the stellar crust and core) can be governed by internal stellar magnetic fields which can affect the neutron star cooling. We plan to study this cooling in a future article.

*Acknowledgements.* We are grateful to A.Y. Potekhin for providing us with the program which calculates the electron chemical potential. Two of the authors (VGB and ADK) acknowledge excellent working conditions and hospitality of N. Copernicus Astronomical Center in Warsaw. This work was supported in part by KBN (grant 2P 304 014 07), RBRF (grant No. 96-02-16870a), INTAS (grant No. 94-3834), and DFG-RBRF (grant No. 96-02-00177G).

## Appendix A

For performing exact quantum calculation of the neutrino synchrotron emissivity from Eq. (2) we replace the integrations over  $p_z$  and  $q_z$  by the integrations over initial and final electron energies  $\varepsilon$  and  $\varepsilon'$ , respectively. In this way we can accurately integrate within the intervals  $|\varepsilon - \mu| \lesssim T$  and  $|\varepsilon' - \mu| \lesssim T$ , where the Fermi-Dirac distributions are rapidly varying. It is also convenient to set  $q_\perp^2 = (\omega^2 - q_z^2)(1 - \eta)$  and replace the integration over  $q_\perp$  by the integration over  $\eta$ . Then

$$Q_{\text{syn}} = \frac{G_F^2 b}{6(2\pi)^5} \sum_{n=1}^{\infty} \int_{\varepsilon_n}^{\infty} \frac{d\varepsilon}{\sqrt{\varepsilon^2 - \varepsilon_n^2}} f \times \sum_{s=1}^n \int \frac{d\varepsilon'}{\sqrt{\varepsilon'^2 - \varepsilon_{n'}^2}} \omega (\omega^2 - q_z^2)^2 D(1 - f'),$$

$$D = \int_0^1 d\eta (C_+^2 R_+ - C_-^2 R_-),$$

$$R_+ = \{1 + \eta [1 + p_\perp^2 + p_z^2 - (\omega^2 - q_z^2) \eta]\} \Psi - [1 + (p_\perp^2 + p_z^2) \eta] \Phi,$$

$$R_- = (1 + \eta)\Psi - (1 - 2\eta)\Phi. \quad (\text{A1})$$

Here,  $n' = n - s$  ( $s$  enumerates cyclotron harmonics);  $\varepsilon_n = \sqrt{1 + 2nb}$  and  $\varepsilon_{n'} = \sqrt{1 + 2n'b}$  correspond to the excitation (de-excitation) thresholds of the initial and final electron states, respectively. The neutrino pair energy and longitudinal momenta are determined from conservation laws:  $p_z = \sqrt{\varepsilon^2 - \varepsilon_n^2}$  and  $p'_z = \pm \sqrt{\varepsilon'^2 - \varepsilon_{n'}^2}$ . The sign of  $p'_z$  and the domain of integration over  $\varepsilon'$  are specified by the minimum longitudinal momentum of the final-state electron for given  $n, \varepsilon$  and  $s$ :

$$p'_1 \leq p'_z \leq p'_2, \quad p'_{1,2} = \pm \frac{\varepsilon_{n'}^2 - (\varepsilon \mp p_z)^2}{2(\varepsilon \mp p_z)} \quad (\text{A2})$$

If  $p'_1 \geq 0$ , one has  $p'_z = \sqrt{\varepsilon'^2 - \varepsilon_{n'}^2}$  and  $\varepsilon'_1 \leq \varepsilon' \leq \varepsilon'_2$ , where

$$\varepsilon'_{1,2} = \frac{\varepsilon_{n'}^2 + (\varepsilon \mp p_z)^2}{2(\varepsilon \mp p_z)}. \quad (\text{A3})$$

If  $p'_1 < 0$ , then there are two integration domains. The first one is  $\varepsilon_{n'} \leq \varepsilon' \leq \varepsilon'_1$ , with  $p'_z = -\sqrt{\varepsilon'^2 - \varepsilon_{n'}^2}$ . The second domain is  $\varepsilon_{n'} \leq \varepsilon' \leq \varepsilon'_2$ , with  $p'_z = \sqrt{\varepsilon'^2 - \varepsilon_{n'}^2}$ .

## Appendix B

Consider the  $z \rightarrow 0$  asymptote of the function  $S_{\text{BC}}(z)$  given by Eq. (12). The integrand of (12) contains the factor  $R = \omega^2 / (\exp(\omega/T) - 1)$ . Since the neutrino-pair energy  $\omega = q_z \cos \theta + s\omega_B^*$  varies near the saddle point, we have

$$R(\omega) = R(\omega_0) + R' \Delta\omega + \frac{1}{2} R'' \Delta\omega^2, \quad (\text{B1})$$

where  $\omega_0 = \kappa_z + s\omega_B^*$  is the value of  $\omega$  in the saddle point,  $\Delta\omega = \cos \theta (q_z - \kappa_z)$ ,

$$R'' = \frac{2 + e^v(-4 + 4v + v^2) + e^{2v}(2 - 4v + v^2)}{(e^v - 1)^3}, \quad (\text{B2})$$

$v = \omega_0/T$ , and  $\kappa_z = s\omega_B^* \cos \theta / \sin^2 \theta$  is the  $z$ -coordinate of the saddle point. The term in (B1), which is linear in  $\Delta\omega$ , does not contribute to (12) due to integration over  $q_z$ .

In the low- $z$  limit (i.e., for  $T \gg T_B$ ), the Bessel functions  $J_s(x)$  and  $J'_s(x)$  in (13) can be expressed through McDonald functions  $K_{1/3}(\eta)$  and  $K_{2/3}(\eta)$  of the argument  $\eta = (s/3)\epsilon^{3/2}$ , where  $\epsilon = 1 - (x/s)^2 = 1 - (q_\perp/\kappa_\perp)^2$ ;  $\kappa_\perp = \omega_B^* s / \sin \theta$  is the coordinate of the saddle point transverse to the magnetic field. These expressions can be written as (Sokolov & Ternov 1974)

$$J_s(x) = \frac{\sqrt{\epsilon}}{\pi\sqrt{3}} \left[ K_{1/3} + \frac{\epsilon}{10} (K_{1/3} - 6\eta K_{2/3}) \right],$$

$$J'_s(x) = \frac{\epsilon}{\pi\sqrt{3}} \left[ K_{2/3} + \frac{\epsilon}{5} \left( 2K_{2/3} - \left( \frac{1}{3\eta} + 3\eta \right) K_{1/3} \right) \right]. \quad (\text{B3})$$

KLY took into account the main terms of these asymptotes. Here, we include small corrections (proportional to the factor  $\epsilon \lesssim s^{-2/3} \ll 1$  in square brackets). This yields

$$\Psi - \Phi = \frac{2\epsilon^2}{3\pi^2} \left[ K_{1/3}^2 + K_{2/3}^2 + \frac{\epsilon}{5} \left( 6K_{1/3}^2 + 4K_{2/3}^2 - 2K_{1/3}K_{2/3} \left( \frac{1}{3\eta} + 6\eta \right) \right) \right]. \quad (\text{B4})$$

Let us substitute (B1) and (B4) into (12). Then

$$S_{\text{BC}}(z) = 1 + a_1 z^{2/3} + a_2 z^{2/3} = 1 - 0.4535 z^{2/3}. \quad (\text{B5})$$

In this case,  $a_1 = L_1 M_1 N_1 / (10 I_0) = 0.2053$  comes from variation of  $\omega$ , with

$$L_1 = \int_0^\pi d\theta \sin^{5/3} \theta \cos^2 \theta = 0.45890,$$

$$M_1 = 3^{2/3} \int_0^\infty dv R'' v^{10/3} = 3^{2/3} \times 76.533,$$

$$N_1 = \int_0^\infty d\eta \eta^{8/3} (K_{1/3}^2 + K_{2/3}^2) = 0.76706,$$

$$I_0 = \frac{8}{3} \pi^2 \zeta(5). \quad (\text{B6})$$

Furthermore,  $a_2 = L_2 M_2 N_2 / (5 I_0) = -0.6588$  comes from the corrections to the McDonald functions,

$$\begin{aligned} L_2 &= \int_0^\pi d\theta \sin^{5/3} \theta = 1.6826, \\ M_2 &= 3^{2/3} \int_0^\infty dv \frac{v^{10/3}}{e^v - 1} = 20.468, \\ N_2 &= \int_0^\infty d\eta \eta^{8/3} \left[ 6K_{1/3}^2 + 4K_{2/3}^2 \right. \\ &\quad \left. - 2K_{1/3}K_{2/3} \left( \frac{1}{3\eta} + 6\eta \right) \right] = -2.6082. \end{aligned} \quad (\text{B7})$$

### Appendix C

Consider the neutrino synchrotron radiation by relativistic degenerate electrons in a very strong magnetic field ( $b \gg 1$ ,  $\sqrt{1+2b} > \mu$ ) in which the bulk of electrons populate the ground Landau level. The electron Fermi momentum is then given by  $p_F = 2x^3/(3b)$ , and the chemical potential is  $\mu = \sqrt{1+p_F^2}$ . The number of electrons on the excited Landau levels is exponentially small, and the major contribution to the neutrino emission comes from the electron transitions from the first excited to the ground Landau level. Equation (3) reduces to

$$A = \frac{C_+^2}{\varepsilon \varepsilon'} [(1+b-u_0b)(2bu_0 - 2bu + u) - u] e^{-u}, \quad (\text{C1})$$

where  $u_0 = (\omega^2 - q_z^2)/(2b)$ . Inserting (C1) into (2) we can integrate over  $q_\perp = \sqrt{2bu}$ :

$$\begin{aligned} Q_{\text{syn}} &= \frac{b^2 C_+^2}{3(2\pi)^5} G_{\text{F}}^2 \int_{-\infty}^{+\infty} dp_z \int_{\{u_0>0\}} dq_z \omega f(1-f') \\ &\quad \times \frac{1}{\varepsilon \varepsilon'} \{ (1+b-bu_0)[2bu_0 + 1 - 2b \\ &\quad + (2b - 1 - u_0)e^{-u_0}] + (1+u_0)e^{-u_0} - 1 \}. \end{aligned} \quad (\text{C2})$$

Since the first Landau level is almost empty, we can set  $f \approx \exp(-(\varepsilon - \mu)/t)$ , where  $t = T/(m_e c^2) = T/(5.93 \times 10^9 \text{ K})$ . The neutrino emission is greatly suppressed by the combination of Fermi-Dirac distributions  $f(1-f')$ . These distributions determine a very narrow integration domain which contributes to  $Q_{\text{syn}}$ .

Equation (C2) can be further simplified in the two limiting cases. The first case is  $\mu_c < \mu < \sqrt{1+2b}$ , or  $p_F/2 < b < b_c$ , where  $\mu_c = (1+b)/\sqrt{1+2b}$  and  $b_c = p_F(p_F + \mu)$ . The main contribution into  $Q_{\text{syn}}$  comes from narrow vicinities of two equivalent saddle points  $p_{z0} = \pm[(p_F + \mu)^2 - 2b - 1]/[2(p_F + \mu)]$ ,  $q_{z0} = \mp b/(p_F + \mu)$ . Each point corresponds to the most efficient electron transition in which an initial-state electron descends to the ground Landau level just with the Fermi energy  $\varepsilon'_0 = \mu$ , emitting a neutrino-pair with the energy  $\omega_0 = |q_{z0}|$ . In this case, the energy of the initial-state electron is  $\varepsilon_0 = \mu + \omega_0$ . One has  $u_0 \ll 1$  in the vicinities of the saddle points. Expanding  $\varepsilon$ ,  $\varepsilon'$ , and  $u_0$  in these vicinities in powers of  $(p_z - p_{z0})$  and  $(q_z - q_{z0})$ , we obtain from Eq. (C2)

$$Q_{\text{syn}} = \frac{G_{\text{F}}^2 C_+^2 b^4 (2b+3)t^4}{3(2\pi)^4 p_F^4 (p_F + \mu) H^3 S} \exp\left(-\frac{b}{(p_F + \mu)t}\right), \quad (\text{C3})$$

where  $H = 1 - (b/b_c)$  and  $S = \sin(\pi H)$ .

The second case corresponds to  $\mu < \mu_c$  or  $b > b_c$ . Now the most efficient electron transitions are those in which the initial-state electron is near the bottom of the first Landau level ( $\varepsilon \approx \sqrt{1+2b}$ ,  $p_z^2 \lesssim t\sqrt{1+2b}$ ). Accordingly,  $\omega = \sqrt{1+2b} - \varepsilon'$  and  $u_0 = (1+b - \varepsilon'\sqrt{1+2b})/b$ . The energy of the final-state electron  $\varepsilon' \approx |q_z|$  varies mostly from the maximum energy  $\varepsilon' = (1+b)/\sqrt{1+2b}$  (associated with the minimum allowable neutrino-pair energy  $\omega = b/\sqrt{1+2b}$  at  $u_0 = 0$ ) to the minimum energy  $\varepsilon' = \mu$  allowed by the Pauli principle. One can put  $p_z = 0$  in all smooth functions under the integral (C2), and replace integration over  $q_z$  by integration over  $\varepsilon'$  or over  $u$ , with  $(1-f') = 1$  in the integration domain. The integration is then taken analytically (for  $b \gg 1$ ) yielding

$$\begin{aligned} Q_{\text{syn}} &= \frac{G_{\text{F}}^2 C_+^2 4b^5 \sqrt{2\pi t}}{3(2\pi)^5 (1+2b)^{3/4}} \\ &\quad \times F(u_1) \exp\left(-\frac{\sqrt{1+2b} - \mu}{t}\right), \end{aligned} \quad (\text{C4})$$

where

$$F(u_1) = \frac{u_1^3}{3} - u_1 + 2 - 2e^{-u_1} - u_1 e^{-u_1}, \quad (\text{C5})$$

and  $u_1 = 1 - (\mu/\mu_c)$ . In the limit of  $\mu \rightarrow 1$  we have  $u_1 \rightarrow 1$  and  $F = (4/3) - (3/e)$ . Then Eq. (C4) reproduces the asymptotic expression for the synchrotron neutrino emissivity of electrons from a non-degenerate electron-positron plasma (Eq. (35) of the paper by Kaminker & Yakovlev 1993). In the opposite limit,  $\mu \rightarrow \mu_c$ , we obtain  $u_1 \rightarrow 0$  and  $F \approx u_1^3/6$ .

Both asymptotes, (C3) and (C4), become invalid in a narrow vicinity  $|1 - (\mu/\mu_c)| \approx 0.5|1 - (b/b_c)| \lesssim \sqrt{t}/b^{1/4}$  of the point  $\mu = \mu_c$  or  $b = b_c$ . We propose to extend the asymptotes, somewhat arbitrarily, to the very point  $\mu = \mu_c$  by replacing

$$\begin{aligned} H &\rightarrow \sqrt{\left(1 - \frac{b}{b_c}\right)^2 + \gamma^2}, \quad S \rightarrow \sin\left(\pi - \frac{\pi b}{b_c}\right) + \pi\gamma, \\ u_1 &\rightarrow \sqrt{\left(1 - \frac{\mu}{\mu_c}\right)^2 + \frac{\gamma^2}{4}} \end{aligned} \quad (\text{C6})$$

in Eqs. (C3) and Eq. (C4). These replacements do not affect significantly  $Q_{\text{syn}}$  outside the vicinity of  $\mu = \mu_c$  but produce physically reasonable interpolation within this vicinity. By matching the modified asymptotes at  $\mu = \mu_c$  and implying again  $b \gg 1$  we get  $\gamma = 1.905t^{1/2}b^{-1/4}$ . In this way we obtain a complete set of equations to describe  $Q_{\text{syn}}$  at  $\mu < \sqrt{1+2b}$ .

### References

- Haensel, P., Pichon, B. 1994, A&A, 283, 313  
 Haensel, P., Kaminker, A.D., Yakovlev, D.G. 1996, A&A, 314, 328  
 Itoh, N., Adachi, T., Nakagawa, M., Kohyama, Y., Munakata, H. 1989, ApJ, 339, 354; Erratum: 1990, ApJ, 360, 741  
 Itoh, N., Hayashi, H., Nishikawa, A., Kohyama, Y. 1996, ApJS, 102, 411

- Kaminker, A.D., Yakovlev, D.G. 1981, *Teor. Matem. Fiz.*, 49, 248
- Kaminker, A.D., Yakovlev, D.G. 1993, *JETP* 76, 229
- Kaminker, A.D., Yakovlev, D.G. 1994, *Astron. Zh.* 71, 910
- Kaminker, A.D., Yakovlev, D.G. 1996, *Astron. Lett.* 22, 549
- Kaminker, A.D., Levenfish, K.P., Yakovlev, D.G. 1991, *Astron. Lett.*, 17, 1090
- Kaminker, A.D., Levenfish, K.P., Yakovlev, D.G., Amsterdamski, P., Haensel, P. 1992a, *Phys. Rev.*, D46, 3256
- Kaminker, A.D., Gnedin, O.Yu., Yakovlev, D.G., Amsterdamski, P., Haensel, P. 1992b, *Phys. Rev.*, D46, 4133
- Kaminker, A.D., Yakovlev, D.G., Haensel, P. 1997, *A&A* (in press)
- Landstreet, J.D. 1967, *Phys. Rev.*, 153, 1372
- Lattimer, J.M., Van Riper, K., Prakash, M., & Prakash, M. 1994, *ApJ*, 425, 802
- Negele, J.W., Vautherin, D. 1973, *Nucl. Phys.*, A207, 298
- Nomoto, K., Tsuruta, S. 1987, *ApJ*, 312, 711
- Pethick, C.J., Thorsson, V. 1996, *Nordita Preprint*, No. 96
- Sokolov, A.A., Ternov, I.M. *Relativistic Electron*. Moscow: Nauka, 1974 (in Russian)
- Vidaurre, A., Pérez, A., Sivak, H., Bernabéu, J., Ibáñez, J.M. 1995, *ApJ*, 448, 264
- Yakovlev, D.G. & Kaminker, A.D. 1994. In: *Equation of State in Astrophysics*, G. Chabrier and E.Schatzman, eds., Cambridge University Press, Cambridge, p. 214
- Yakovlev, D.G., Levenfish, K.P. 1995, *A&A*, 297, 717